JOURNAL OF VIROLOGY, Jan. 2010, p. 847–855 Vol. 84, No. 2
0022-538X/10/$12.00 doi:10.1128/JVI.01801-09

Insulin-Degrading Enzyme Binds to the Nonglycosylated Precursor of Varicella-Zoster Virus gE Protein Found in the Endoplasmic Reticulum▽

J. E. Carpenter,[1] W. Jackson,[1] G. A. de Souza,[2] L. Haarr,[2] and C. Grose[1]*

Children's Hospital, University of Iowa, Iowa City, Iowa,[1] and Gade Institute, University of Bergen, Bergen, Norway[2]

Received 26 August 2009/Accepted 20 October 2009

Insulin degradation enzyme (IDE) is a 110-kDa zinc metalloprotease found in the cytosol of all cells. IDE degrades insulin and a variety of small proteins including amyloid-β. Recently, IDE has been proposed as the receptor for varicella-zoster virus (VZV) attachment. During our reassessment, some of the original studies were repeated and expanded in scope. We first confirmed that IDE antibody reduced VZV spread. For additional controls, we repeated the same experiments with herpes simplex virus (HSV)-infected cells as well as uninfected cells. There was a visible reduction in HSV spread but less than seen in the VZV system. Of greater importance, IDE antibody also inhibited the growth of uninfected cells. Second, we repeated the coprecipitation assays. We confirmed that antibodies to VZV gE (open reading frame 68) coprecipitated IDE and that anti-IDE antibody coprecipitated gE. However, the detected gE protein was not the mature 98-kDa form; rather, it was a precursor 73-kDa gE form found in the endoplasmic reticulum. Additional control experiments included VZV-infected cell cultures treated with tunicamycin to block gE glycosylation in the endoplasmic reticulum; again, the anti-IDE antibody coprecipitated a 73-kDa gE product. Finally, Orbitrap mass spectrometry analysis of a chromatographically purified gE sample revealed four cellular proteins associated with the unfolded protein response: BiP (HSPA5), HSPA8, HSPD1, and PPIA (peptidyl-propyl *cis-trans* isomerase). We conclude that IDE protease binds to the 73-kDa gE precursor and that this event occurs in the cytosol but not as a receptor/ligand interaction.

Insulin degradation enzyme (IDE) has been proposed as a virus receptor. IDE is a zinc metalloprotease that is known to degrade a number of small proteins (<6 kDa) including insulin and amyloid-β (6, 18). Because of these observations, IDE has been intensively studied as a participant in the pathogenesis of diabetes and Alzheimer's syndrome (9, 30). In 2006, IDE was reported to be a cellular receptor of varicella-zoster virus (VZV), which mediated infection and cell-to-cell spread of the virus (19). This report was based on several experiments. Initially, a truncated VZV gE protein was immobilized onto protein A-Sepharose beads with anti-gE monoclonal antibody (MAb). When the beads were incubated with cell lysates, a protein identified as IDE was attached to the complex. The authors also performed coimmunoprecipitation assays. When gE was precipitated from VZV-infected melanoma cells, the investigators observed that IDE was also detectable in the precipitate. When a rabbit polyclonal anti-IDE antibody was added to a monolayer prior to VZV infection, VZV spread was subsequently inhibited by 30 to 45%. Knockdown of IDE by small interfering RNA (siRNA) inhibited VZV infection and cell-to-cell spread. Similarly, bacitracin, a compound that inhibits IDE, also inhibited VZV infection and cell-to-cell spread. Finally, these deficiencies were corrected by expression of exogenous IDE. In a subsequent publication, the IDE binding domain in gE was localized to amino acids 32 to 71 (20). Removal of that gE domain from a recombinant virus limited cell spread (1).

In this report, we present additional data about the VZV gE-IDE interaction. We first confirmed the interaction. But we found that the interaction occurred predominantly in the cytosol with a precursor nonglycosylated gE form (73 kDa) rather than the mature gE glycoprotein (98 kDa). In fact, the gE-IDE interaction occurred when VZV-infected cells were treated with tunicamycin to prevent the biosynthesis of mature glycosylated gE. The above results suggested that the VZV gE-IDE interaction may occur either in the endoplasmic reticulum (ER) or adjacent to the ER, a site where IDE is known to interact with other proteins such as amyloid-β.

MATERIALS AND METHODS

Viruses and cells. The VZV-32 strain was first isolated in Texas from a child with chickenpox and is a low-passage laboratory strain. Its genome has been completely sequenced and falls within a European clade (29). Human melanoma cells designated MeWo were the cell substrate. Cells were grown in minimal essential medium with Earle's salts (E-MEM) supplemented with 10% fetal bovine serum (FBS). When cells were nearly confluent, they were inoculated with VZV-infected cells at a ratio of one infected cell to eight uninfected cells by previously described methods (14). In a few experiments, cell-free virus was the inoculum (16). For the experiments with herpes simplex virus type 1 (HSV-1), cells were inoculated with strain F stock at 500 or 1,000 PFU, kindly provided by Richard Roller (8).

Primary and secondary antibody reagents. Reagents for VZV gE included murine MAb 3B3 and a guinea pig monospecific polyclonal antibody; the guinea pig polyclonal antibody to VZV gE was obtained from the serum of a guinea pig immunized twice with gE protein purified by affinity (3B3) chromatography. For HSV-1 gE, a rat polyclonal antibody was obtained from David Johnson (Oregon Health and Science University) (23); for IDE, MAb IDE and a rabbit polyclonal antibody were purchased from Covance, Inc. MAbs 6B5, 258, and 158 from this laboratory detected VZV gI, gH, and gB, respectively (14). Fluorescently tagged

* Corresponding author. Mailing address: University of Iowa Hospital, 200 Hawkins Drive, Iowa City, IA 52242. Phone: (319) 356-2270. Fax: (319) 356-4855. E-mail: charles-grose@uiowa.edu.

▽ Published ahead of print on 28 October 2009.

secondary antibodies were conjugated to the Alexa Fluor 488 and 546 fluoroprobes (Invitrogen).

Immunoprecipitation. Primary antibody (5 μl) was added to 100 μl of infected cell lysate (25 cm^2 of infected cells yields 1 ml of lysate) and diluted with 200 μl of radioimmunoprecipitation assay (RIPA) buffer (150 mM NaCl, 50 mM Tris, 1 mM EDTA, 1 mM phenylmethylsulfonyl fluoride [PMSF], 0.1% Nonidet P-40, 1% deoxycholate [DOC], 0.1% SDS, protease inhibitors (Sigma P8340) adjusted to pH 7.4) and then placed on a rotator at 4°C overnight. Following antibody incubation, 50 μl of Sepharose-protein A beads in protein A storage buffer (150 mM NaCl, 10 mM Tris, pH 7.4) was added to each sample, which was then placed back on the rotator at 4°C for 4 h. The samples were then washed three times (beads were sedimented at 500 rpm for 2 min, supernatant was removed by pipette, and beads were resuspended with RIPA buffer and placed back on the rotator at 4°C for 5 min). After the last wash, the beads were resuspended in 100 μl of SDS reducing sample buffer (60 mM Tris, 10% glycerol, 3% SDS, 10% β mercaptoethanol, pH 6.8), and the samples were placed in boiling water for 10 min. After cooling, the beads were sedimented at 500 rpm for 2 min, and the supernatant was removed to another tube for later use.

Immunoblotting. Antigens within viral material lysates or immunoprecipitates were prepared for immunoblotting by previously described techniques using a SuperSignal chemiluminescent kit (Pierce) (32). The protein component of the lysate was separated by SDS-PAGE using 10 or 12% acrylamide gels, transferred to a polyvinylidene difluoride (PVDF) membrane and blotted with primary antibody diluted 1:2,000 to 1:10,000 in 1% nonfat milk in phosphate-buffered saline (PBS) with 0.1% Tween 20 (T-PBS) for 1 h after being blocked for 1 h in 5% nonfat milk. After three washes with T-PBS, the membrane was incubated in secondary antibody conjugated to horseradish peroxidase diluted 1:40,000 in 1% nonfat milk in T-PBS for 1 h at room temperature (RT). After five washes with T-PBS, the membrane was soaked in a chemiluminescent solution (peroxide-luminol) from Pierce for 5 min, blotted dry, and then exposed to X-ray film for various durations from 5 s to 12 h.

Immunolabeling. Infected and uninfected control cells were fixed and permeabilized with 2% paraformaldehyde and 0.05% Triton X-100 in 0.15 M phosphate-buffered saline, washed with PBS three times for 5 min, and then incubated with 5% nonfat milk in PBS for 1 h. Subsequently, the samples were incubated with one of the primary MAbs diluted 1:1,000 to 1:2,000 in 1% nonfat milk in PBS at RT for 1 h. After three rinses for 5 min each in PBS, the samples were treated with the appropriate secondary antibody diluted 1:1,250 in 1% nonfat milk in PBS and incubated at RT for 1 h. The specimens were subsequently rinsed three times for 5 min with PBS.

Confocal microscopy. Our methods for confocal microscopy have been extensively described previously (7, 28). Following immunostaining with fluorescent secondary antibody (Molecular Probes) and rinsing with PBS, the coverslips were turned over onto a drop of H-1200 Vectashield (Vector Labs) on a glass slide and then sealed in place with nail polish. After the samples hardened, they were directly viewable on a Zeiss 510 confocal microscope.

Immunoabsorbent chromatography. Generation of a VZV gE-specific affinity chromatography column followed our previously described method (10). Briefly, 20 mg of MAb 3B3 was added to 10 ml of cyanogen bromide (CnBr)-activated Sepharose 4B beads (1.2 g of dry beads from Sigma swollen with 10 ml of 0.1 mM HCl and then activated with high-pH borate buffer [0.1 M sodium borate, 0.5 M NaCl, pH 8.3]) and rotated for 1 h at RT. The reaction was quenched with 1 M Tris (pH 8.0), beads were sedimented, and supernatant was removed. The beads were then incubated with 0.1 M Tris, pH 8.0, overnight at 4°C and then washed twice with the following (in order): 25 ml of buffer A (50 mM NaCl, 2 mM EDTA, 5 mM NaN_3, 10% glycerol, pH 11), 25 ml of PBS, 25 ml of buffer B (0.5 M NaCl, 0.1 M sodium acetate, pH 4.0), and finally 25 ml of PBS. Monolayers of infected cells (1,350 cm^2) were lysed with 35 ml of RIPA buffer and dislodged into PBS yielding 75 ml of lysate. The 3B3-linked Sepharose 4B beads were added to 75 ml of lysate and rotated overnight at 4°C. The beads were sedimented, supernatant was removed and then transferred back into a 10-ml column, and samples were washed with 75 ml of PBS augmented with 0.5% NP-40 to remove any remaining amount of unbound lysate. VZV gE protein was eluted into 2-ml fractions, using 7.7 mg of the peptide DQRQYGDVFKGD, corresponding to the gE 3B3 epitope, dissolved in 25 ml of PBS.

Mass spectrometry. For our analyses, 10 μg per replicate of sample was reduced using 10 mM dithiothreitol (DTT) for 1 h at 56°C and alkylated with 55 mM iodoacetamide for 45 min at ambient temperature. After that, the sample was diluted 1:5, vol/vol, in 100 mM ammonium bicarbonate and digested with 2% trypsin (sequence grade modified; Promega) for 16 h at 37°C at pH 8.0. The reaction was quenched through acidification with 2% trifluoroacetic acid (Fluka). The resulting peptide mixture was desalted using reverse-phase C_{18} stop and go extraction (STAGE) tips and diluted in 0.1% trifluoroacetic acid prior to nano-high-performance liquid chromatography-mass spectrometry (HPLC-MS) analysis (31). Prior to injection in the spectrometer, the samples were separated by liquid chromatography using an Acclaim PepMap 100 column (C_{18}, 3-μm particle size, and 100-Å pore size; Dionex Corp.) with a capillary bed length of 12 cm, an internal diameter of 100 μm, and self-packed with Reprosil-Pur C18-aq (Maisch GmbH). The gradient was 7% solvent B to 40% solvent B in 87 min, followed by 40 to 80% solvent B in 8 min. Solvent A was aqueous 2% acetonitrile in 0.1% formic acid, whereas solvent B was aqueous 90% acetonitrile in 0.1% formic acid.

All experiments were performed on a Dionex Ultimate 3000 nano-LC system connected to a linear quadrupole ion trap (LTQ)-Orbitrap mass spectrometer (ThermoElectron) equipped with a nanoelectrospray ion source (34). The mass spectrometer was operated in data-dependent mode to automatically switch between Orbitrap-MS and LTQ-tandem MS (MS/MS) acquisition. Full-scan MS spectra (from m/z 300 to 2,000) were acquired in the Orbitrap with resolution (R) of 60,000 at m/z 400 (after accumulation to a target of 1,000,000 charges in the LTQ). For accurate mass measurements the "lock mass" option was enabled in MS mode, and polydimethylcyclosiloxane (PCM) ions generated in the electrospray process from ambient air were used for internal recalibration during the analysis (27). Target ions already selected for MS/MS were dynamically excluded for 60 s. General mass spectrometry was conducted with an electrospray voltage of 1.5 kV, no sheath, and auxiliary gas flow. The ion selection threshold was 500 counts for MS/MS, and an activation Q-value of 0.25 and activation time of 30 ms were also applied for MS/MS.

MS/MS peak lists from individual RAW files were generated using the DTA SuperCharger package, version 1.29, available in the MSQuant validation tool. We used Mascot Daemon for multiple search submissions on a local Mascot server, version 2.1 (Matrix Science) (4, 5). Under our criteria, Mascot indicated a minimal score of 31 for a P value of ≤ 0.05. All data had a mass accuracy average of 3.1 ppm.

RESULTS

Inhibition of VZV and HSV-1 cell spread by an IDE antibody. One of the key observations in the original report was that incubating VZV-infected melanoma cells with an IDE antibody at 1:100 inhibited VZV cell spread (19). We repeated this experiment with a cell-free virus inoculum and found that VZV cell spread was markedly reduced by the IDE antibody compared with control medium or medium containing a 1:100 concentration of preimmune rabbit serum (Fig. 1). VZV-infected cells incubated with IDE antibody showed virtually no cytopathic effect (Fig. 1E and F) while widespread VZV gE was evident in infected cells incubated in control medium or medium containing preimmune rabbit serum (Fig. 1A to D). We next repeated the same experiment looking at HSV-1 cell spread. Specifically, melanoma cells in 24-well plates were infected with HSV-1 at 500 PFU or 1,000 PFU and incubated in either 1:100 IDE antibody or 1:100 preimmune rabbit serum for 24 h; cells were then fixed, stained with crystal violet, and examined with an optical microscope (Fig. 2). Clearly, the well containing cells incubated with the IDE antibody showed fewer plaques of smaller size than wells containing cells incubated in normal medium or medium with 1:100 preimmune rabbit serum (Fig. 2A). Sizes of each plaque were measured with NIH ImageJ software (http://rsb.info.nih.gov/nih-image/). The sizes of all plaques were then summed to assess the extent of HSV cell spread. The well incubated in IDE antibody showed 60% less plaque area than the well incubated with normal rabbit serum in infections at either 500 PFU or 1,000 PFU (Fig. 2B). The latter result suggested that incubation with IDE antibody may diminish the ability of melanoma cells to host viral infection.

Inhibition of melanoma cell growth by an IDE antibody. To pursue the hypothesis that incubation with the IDE antibody

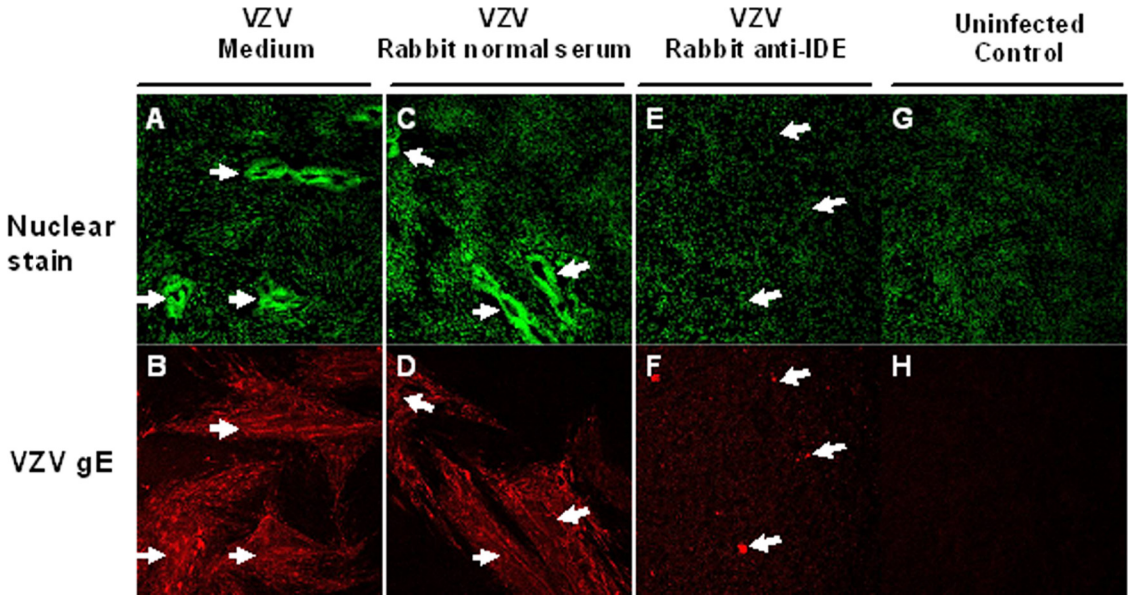

FIG. 1. Inhibition of VZV cell spread by IDE antibody. MeWo cells were incubated with complete medium only (A and B; G and H) or rabbit preimmune serum at 1:100 in complete medium (C and D) or rabbit polyclonal IDE antibody at 1:100 in complete medium (E and F) for 1 h at 4°C. Cell-free VZV-32 virus was added to wells A, B, C, D, E, and F. Wells G and H were uninfected controls. Cultures were then incubated at 32°C for 72 h, fixed for 1 h in 2% paraformaldehyde containing 0.05% Triton X-100, and stained with Pico Green (A, C, E, and G) and anti-gE MAb 3B3 (B, D, F, and H). White arrows indicate foci of infection.

may be directly affecting the metabolism of the melanoma cells used to host viral infection in cell culture, we investigated the multiplication of MeWo cells incubated with the IDE antibody. Specifically, we split MeWo cells in half and then allowed them to grow to confluence over 72 h while being incubated with control medium or medium treated with a 1:100 dilution of a rabbit polyclonal antibody to IDE or a MAb to IDE. Triplicate samples were fixed at 48 and 72 h postplating and then stained with a nuclear stain. At least 10 images at a magnification of ×200 were taken at random locations within each well, resulting in almost 600 images, each containing 300 to 600 nuclei. Cellular density was then calculated by enumerating the number of nuclei in each image. The density of cells in wells incubated with IDE antibodies was about 20% less than the density in the control wells by 72 h (Fig. 3). This result supported the hypothesis that incubation of melanoma cells with IDE antibody diminished the ability of the cells to grow and likely diminished their ability to host viral infection.

Coprecipitation of individual VZV glycoproteins with IDE. Another key observation in the original report was that IDE coprecipitated with VZV gE but not with other VZV glycoproteins (19). We set out in an initial series of experiments to confirm this observation by screening VZV glycoproteins gE, gI, gH, and gB for binding to IDE by precipitating the glycoproteins with their respective monoclonal antibodies and then blotting the precipitates for IDE using the rabbit polyclonal antibody. Only gE and, to a minor extent, gI coprecipitated IDE (Fig. 4). It is likely that the minor extent of gI precipitation was due to the complex gI forms with gE (12). To further refine this observation, we precipitated IDE from VZV-infected cell lysates using two different gE antibodies, the same MAb 3B3 used in the experiment shown in Fig. 1 or a guinea pig-monospecific polyclonal antibody, and again blotted for IDE. Both antibodies coprecipitated IDE (Fig. 5). Confirming the earlier report, IDE and gE bound together in infected cell lysates. Since the gE-IDE interaction may not occur at the cell surface, based on data shown in Fig. 3, we postulated that IDE may attach to a partially processed gE form in the cytosol.

Coprecipitation of VZV gE or HSV gE with IDE. To consider this question and also investigate the specificity of the interaction, we carried out coprecipitation experiments between IDE and gE from both VZV and HSV-1. First, precipitating with antibodies against HSV gE and then blotting for IDE showed that HSV-1 gE did not coprecipitate IDE to the same extent as VZV gE (Fig. 6B, lanes 1 and 3). This result was confirmed in the reverse coprecipitation experiment, i.e., precipitating with an IDE antibody and blotting for gE. The blot showed that HSV-1 gE was not coprecipitated with IDE. Surprisingly, the dominant form of coprecipitated VZV gE had a lower molecular weight (MW) than the mature form (Fig. 6A, lanes 3 and 4). The antibody used in the blot for VZV gE was MAb 3B3. Its epitope has been mapped between residues 150 to 162 on the gE ectodomain (32). Given the surprising result, this experiment was repeated six times with the same result. The result was the same with the high-titered guinea pig polyclonal monospecific gE antiserum used in the experiment shown in Fig. 5. In all experiments, the precursor 73-kDa gE form was the most prominent precipitated protein.

Coprecipitation of the 73-kDa precursor gE with IDE under different salt conditions. We have used MAb 3B3 in numerous VZV gE experiments published over the past 25 years, and this reagent has invariably immunoblotted all gE forms present in an infected culture (11). Because the result shown in Fig. 6 was completely unexpected, we tested whether the VZV gE profile would be different if we varied the salt concentration in our precipitation reaction. To this end, we carried out the precip-

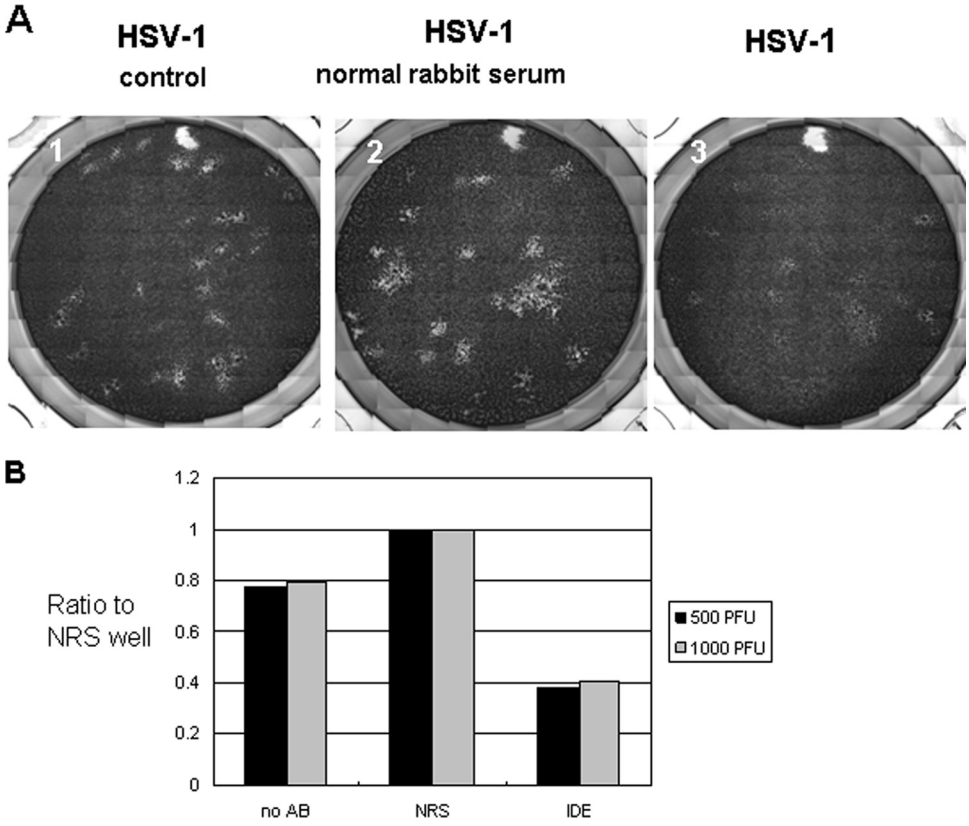

FIG. 2. Inhibition of HSV-1 cell spread by IDE antibody. (A) MeWo cells were incubated with complete medium only (frame 1) or preimmune (normal) rabbit serum (NRS) at 1:100 in complete medium (frame 2) or rabbit anti-IDE antibody at 1:100 in complete medium (frame 3) for 1 h at 4°C. HSV-1 (F strain) stock was added to two sets of three wells under different incubation conditions, one at 500 PFU and the other set at 1,000 PFU (500 PFU shown). Cultures were then incubated at 32°C for 24 h. Cells were fixed for 1 h in 2% paraformaldehyde in PBS and then stained with crystal violet. Optical images at a magnification of ×40 were combined into a montage of the whole well. (B) Plaques in each well were counted, and their sizes were measured by NIH ImageJ using the Freehand tool. The extent of cellular spread was determined by adding the sizes of all plagues in each well. For each inoculum, the calculated cellular spread was normalized to the value obtained for the well incubated in normal rabbit serum in panel A. Together, the data showed that incubation with IDE antibody inhibited HSV-1 cellular spread by 60%.

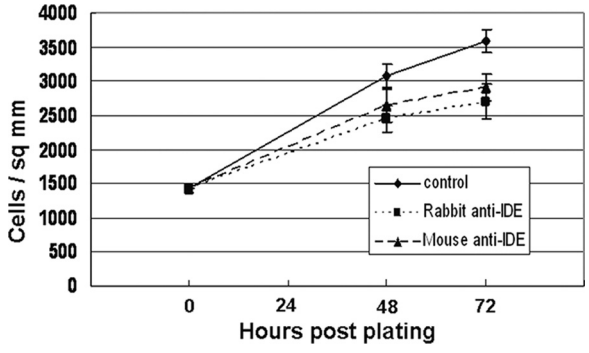

FIG. 3. Inhibition of melanoma cell proliferation by IDE antibodies. Melanoma cells were split at a ratio of 1:2.5 into two 24-well plates; three wells each were incubated in 1:100 rabbit polyclonal IDE antibody or 1:100 mouse MAb to IDE; six wells were incubated normally as the control. At 48 and 72 h postplating, the cells were fixed and stained with the PicoGreen stain. Ten images at a magnification of ×200 were taken in random positions within each well, and nuclei were counted in each image. The error bars correspond to the 95% confidence interval. Growth of melanoma cells was significantly reduced by incubation with IDE antibodies.

itation of IDE from infected cell lysates using buffers with twice or half the amount of normal (isotonic) salt, after which we again blotted for VZV gE. We found that high salt abolished the coprecipitation completely while low salt accentuated the interaction between the 73-kDa form of gE and IDE; in addition, at lower salt concentrations, the higher-molecular-weight forms of gE were precipitated in small amounts (Fig. 7).

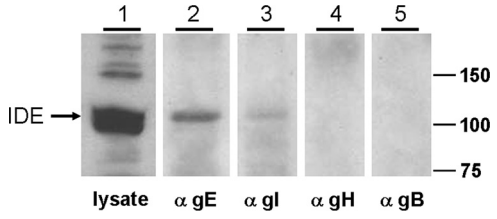

FIG. 4. Coprecipitation of IDE by VZV glycoprotein antibodies. VZV-infected cell lysate was generated from VZV-infected cultures at 72 h postinfection. VZV glycoproteins gE, gI, gH, and gB were immunoprecipitated from the VZV lysate using MAbs 3B3, 6B5, 258, and 158, respectively. The precipitates were separated by SDS-PAGE and subjected to Western blotting for IDE (lanes 2 to 5). Lane 1 is a Western blot of IDE directly from VZV lysate. α, anti.

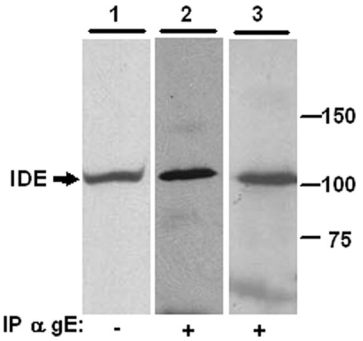

FIG. 5. Coprecipitation of IDE by different anti-gE antibodies. VZV-infected cell lysate was generated from VZV-infected cultures at 72 h postinfection. VZV gE was immunoprecipitated (IP) from the VZV lysate using two different antibodies: murine MAb 3B3 (lane 2) and guinea pig polyclonal antibody to gE (lane 3). The precipitates were separated by SDS-PAGE and subjected to Western blotting for IDE (lanes 2 to 3). Lane 1 is a Western blot of IDE directly from VZV lysate. α, anti.

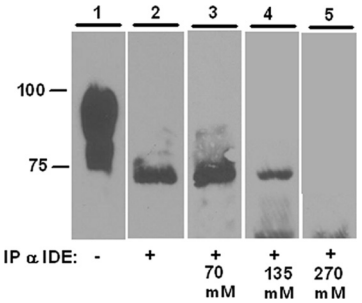

FIG. 7. Effect of salt concentration on the coprecipitation of VZV gE by an IDE antibody. VZV-infected cell lysate was generated from VZV-infected cultures at 72 h postinfection. IDE was immunoprecipitated (IP) from VZV lysate using a rabbit polyclonal antibody (Covance) with buffers containing various concentrations of salt. The precipitates were separated by SDS-PAGE and subjected to Western blotting for VZV gE using MAb 3B3. Lane 3 corresponds to the lowest salt concentration (70 mM), lane 4 corresponds to normal (isotonic) salt concentration (135 mM), and lane 5 corresponds to the highest salt concentration (270 mM). Lane 1 is a lysate control to demonstrate that all forms of gE were present in the lysate, and lane 2 is another 73-kDa gE precipitate control under standard conditions as described in Materials and Methods. α, anti.

This finding is relevant because prior investigators used a low concentration of salt (10 times lower than normal) in their immunoprecipitation buffer (19). Our results suggested that higher-molecular-mass forms of gE, including the mature 98-kDa form, would coprecipitate with IDE at a very low salt concentration. Nevertheless, the 73-kDa form was still the most prominent.

Coprecipitation between VZV gE and IDE in tunicamycin-treated infected cells. In an earlier characterization of gE maturation, we analyzed gE in infected cultures treated with tunicamycin (24). Tunicamycin is a mixture of antibiotics which inhibits formation of polyisoprenyl *N*-acetylglucosaminyl pyrophosphates (38). In other words, tunicamycin blocks the formation and attachment of mature N-linked glycans onto a polypeptide backbone. We had previously documented the prominence of a 73-kDa gE protein in cultures treated with tunicamycin. Therefore, we postulated that IDE preferentially bound to the same precursor gE form as that seen in the coprecipitation experiments presented above. To test this hypothesis, we again treated VZV-infected cultures with tunicamycin under the same conditions as previously described and repeated the coprecipitation experiments exactly as described above. When the tunicamycin-treated extract was precipitated with IDE antibody, subjected to SDS-PAGE, and immunoblotted with anti-gE antibody, the precursor 73-kDa gE form was detected (Fig. 8A). Furthermore, if the dominant 73-kDa form of gE in the tunicamycin-treated infected cell lysate was precipitated with a gE antibody and then blotted for IDE, IDE was coprecipitated with the immature form of gE (Fig. 8B).

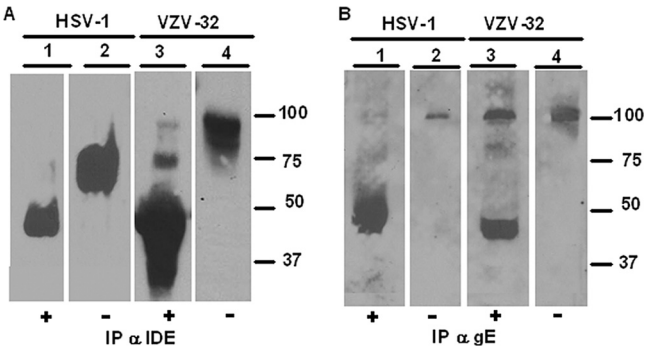

FIG. 6. Coprecipitation of IDE with VZV gE and HSV-1 gE. VZV- and HSV-1-infected cell lysates were generated from VZV- and HSV-1-infected cultures at 72 h postinfection and 24 h postinfection, respectively. (A) IDE was immunoprecipitated (IP) from the respective lysates using a rabbit polyclonal antibody (Covance). The precipitates were separated by SDS-PAGE and subjected to Western blotting for HSV-1 gE using a rat MAb (lane 1) and for VZV gE using the mouse MAb 3B3 (lane 3). Lanes 2 and 4 are Western blots of gE directly from HSV-1 and HSV lysates. The major bands less than 50 kDa corresponded to the IDE antibody used in the precipitation. (B) VZV and HSV-1 gE were immunoprecipitated (IP) from the respective lysates using the mouse MAb 3B3 to VZV gE and a rat MAb to HSV-1 gE. The precipitates were separated by SDS-PAGE and subjected to Western blotting for IDE (lanes 1 and 3) using the mouse MAb to IDE (Covance). Lanes 2 and 4 are Western blots of IDE directly from HSV-1 and VZV lysates. Note prominent IDE blot in VZV lane 3. The major bands less than 50 kDa corresponded to the gE antibodies used in the precipitation. α, anti.

VZV gE trafficking in tunicamycin-treated infected cells. In our prior gE biochemical studies with tunicamycin, we had never performed an imaging analysis of gE trafficking after tunicamycin treatment. To complete this aspect of our earlier research, we performed a confocal microscopy survey of gE trafficking with and without tunicamycin. Tunicamycin was added 5 h after infection, and the cultures were incubated for another 24 h. Then the monolayers were fixed, immunolabeled, and imaged by confocal microscopy (Fig. 9). The results clearly demonstrated that gE, in the presence of tunicamycin, was blocked in its transit out of the ER en route to the Golgi compartment (Fig. 9A). In contrast, gE trafficking through the cytoplasm to the plasma membrane was easily detected in the nontreated cultures (Fig. 9B). These images were in complete agreement with our prior biochemical analyses. We also observed during these imaging experiments that murine MAb 3B3 immunostained gE trapped within the ER more intensely

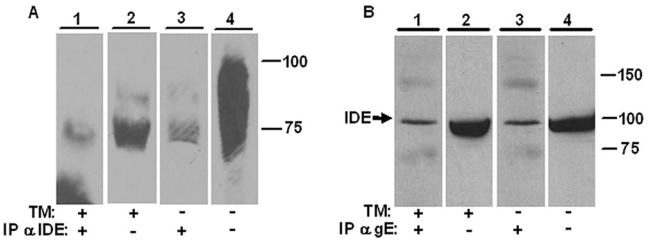

FIG. 8. Coprecipitation of VZV gE and IDE in tunicamycin-treated VZV-infected cell cultures. Tunicamycin-treated VZV lysate was generated from VZV-infected melanoma cells incubated in medium containing 2.5 μg/ml tunicamycin for 24 h starting at 5 h postinfection. Untreated VZV lysate was generated from VZV-infected cells at 72 h postinfection. (A) IDE was immunoprecipitated (IP) from the treated and untreated lysates using a rabbit polyclonal antibody (Covance). The precipitates were separated by SDS-PAGE and subjected to Western blotting for VZV gE using the mouse MAb 3B3. Lanes 1 and 3 are the blots of the precipitates from the treated and untreated lysates. Lanes 2 and 4 are Western blots of gE directly from VZV-treated and untreated lysates. The lanes show that the precursor form of gE at 73 kDa was pulled down from untreated and treated lysates. Lane 2 shows that only the 73-kDa form was present in the treated lysate. (B) VZV gE was immunoprecipitated from both treated and untreated lysates using a guinea pig polyclonal antibody to VZV gE. The precipitates were separated by SDS-PAGE and subjected to Western blotting for IDE (lanes 1 and 3) using a mouse MAb to IDE (Covance). Lanes 2 and 4 are Western blots of IDE directly from treated and untreated VZV lysates. The lanes show that IDE was coprecipitated with VZV gE from both treated and untreated VZV-infected cell lysates even though only the 73-kDa form of gE was present in the treated lysate. α, anti.

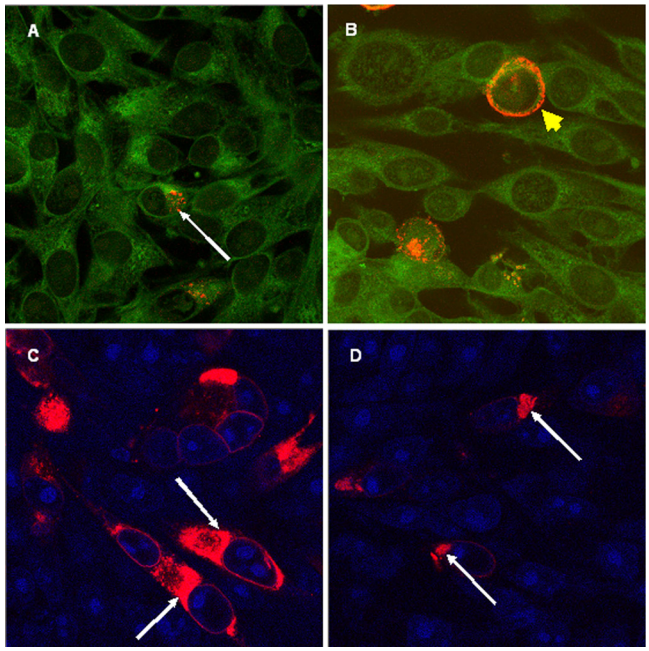

FIG. 9. Localization of VZV gE in the ER of tunicamycin-treated VZV-infected cells. MeWo cells were infected with VZV-32 and incubated at 32°C for 5 h. Then, the medium was removed from the infected cells and replaced with complete medium containing 2.5 μg/ml tunicamycin (A, C, and D) or complete medium without tunicamycin (B). Monolayers were incubated for another 24 h. Thereafter, the infected cells shown in panels A and B were stained with 0.7 mg/ml of 3,3′-dihexyloxa-carbocyanine iodide (DiOC) in 95% ethanol for 10 min at 37°C in the dark. The DiOC-labeled cells (green) were fixed and permeabilized with Triton X-100 and then incubated with guinea pig anti-VZV gE, followed by goat anti-guinea pig secondary antibody conjugated to a red fluorophore (A and B). Panels C and D were fixed and permeabilized and incubated with the nuclear stain Toto-3 iodide (blue) and a red anti-gE MAb 3B3 (C) or a red guinea pig anti-gE (D). Note the presence of red gE staining in the outer cell membrane only in panel B (yellow arrow). White arrows indicate areas of gE (red) localization in the ER in panels A, C, and D. Samples were imaged at a magnification of ×100.

than the guinea pig anti-gE antibody (compare Fig. 9C and D). This conclusion was reached after observing several Z-stacks of images (data not shown); Fig. 9 represents one slice of each Z-stack. In summary, IDE coprecipitated with an immature form of VZV gE that was largely localized in the ER.

Proteomics analysis of VZV gE binding partners. The fact that IDE interacted predominantly with the gE 73-kDa form found in the ER led to a further hypothesis. Namely, the gE-IDE interaction occurred in the cytoplasm at a site in or adjacent to the ER, possibly secondary to ER stress (39). We have previously documented that VZV glycoproteins are produced in such abundance in infected cultures and that biosynthesis of cellular glycoproteins is no longer detectable with radio sugar labeling (13). The overabundant production of glycoproteins within a cell is a well-known precipitant of ER stress (25).

To test for evidence of ER stress, we first purified the gE glycoprotein by immunoabsorbent chromatography and then analyzed this fraction by Orbitrap mass spectrometry (21, 34). This high-accuracy instrument uses a variation of ion cyclotron technology whereby the fragmented ions spiral down the length of the magnet (4, 5). The radius of the spiral is related to the mass/charge ratio. Ion cyclotron mass spectrometers exhibit very high mass discrimination due to the large number of orbits sampled (22). In addition to the detection of the gE protein and its complex partner gI, a number of other viral and cellular proteins were detected in the purified fraction (Table 1). Interestingly, IDE was not detected. Included in the set of detected cellular proteins were four members of the unfolded protein response (UPR) (2, 25). These included heat shock proteins HSPA5 (BiP), HSPA8, and HSPD1. The fourth protein was PPIA (peptidyl-propyl *cis-trans* isomer catalyst). The last results suggested that misfolded VZV gE was a candidate protein for ER retrotranslocation.

DISCUSSION

We have reexamined the previously described interaction of VZV gE and IDE and concur that IDE binds a gE product and that treatment of VZV-infected cells with an IDE antibody greatly inhibits cell-to-cell spread of the virus (19). However, we found that IDE primarily bound the 73-kDa unglycosylated gE form and that incubation with IDE antibodies also inhibited cell-to-cell spread of HSV-1 as well as the growth of uninfected melanoma cells. These observations have led us to hypothesize that IDE and the precursor gE form interact in the cytosol, most likely as a consequence of ER stress, and that the observation that IDE antibody inhibits VZV cell-to-cell spread is a separate and unrelated phenomenon. We suggest that treatment with IDE antibodies inhibits the function of IDE

TABLE 1. Proteins identified by mass spectrometry in VZV-infected cell lysate purified by affinity chromatography[a]

Gene or protein	Description	No. of MS peaks[b]	Avg Mascot score[c]
ORF68	Envelope glycoprotein E (human herpesvirus 3)	32	66
ORF67	Envelope glycoprotein I (human herpesvirus 3)	17	55
ORF9	Tegument protein VP22 (human herpesvirus 3)	5	54
ORF62	Human herpesvirus 3	3	68
ORF31	Envelope glycoprotein B (human herpesvirus 3)	3	50
ORF40	Major capsid protein (human herpesvirus 3)	1	76
ORF65	Membrane protein US9 (human herpesvirus 3)	1	72
VIM	Vimentin	17	59
ACTB	Actin, cytoplasmic	8	60
TUBB	Tubulin beta chain	5	56
SLC3A2	Solute carrier family 3	2	55
MYL6	MYL6B nonmuscle isoform of myosin light polypeptide 6	2	53
PPIA	Peptidyl-prolyl *cis-trans* isomerase A	2	46
HSPA8	Isoform 1 of 71-kDa heat shock protein	2	42
ACTN1	Alpha-actinin-1	1	78
CFL1	Cofilin-1	1	77
TUBA1C	TUBA1C protein	1	76
HSPA5	HSPA5 protein	1	74
HSPD1	60-kDa Heat shock protein	1	72
TPM3	Isoform 2 of tropomyosin alpha-3 chain	1	70

[a] VZV-infected cell lysate was generated from VZV-infected cultures at 72 h postinfection. The lysate was passed through an affinity column packed with Sepharose 4B beads conjugated to an anti-gE MAb. After a washing step, bound proteins were eluted in a high-salt solution and purified for injection by electrospray into an LTQ-Orbitrap mass spectrometer (Thermoelectron). The resulting mass/charge spectrum was normalized and searched against viral and human protein databases using Mascot. The table includes 7 viral and 13 cellular proteins. Cellular proteins associated with the unfolded protein response are shown in bold type.

[b] Data are for peaks corresponding to peptides that were matched to the proteins.

[c] Data are for all matched peptides. A score above 31 indicates a match significance P value of <0.05.

within the cell. The consequences of this inhibition are difficult to predict. Shii et al. found that microinjection of a monoclonal antibody to IDE into hepatoma cells inhibited insulin degradation by an average of 39% (35). More recently, Chou et al. found that IDE interacts with the intermediate filament proteins vimentin and nestin (3). In turn, vimentin and nestin can either activate or suppress the proteolytic IDE activity, depending upon substrate. Thus, any antibody-mediated inhibition of IDE activity would have unpredictable consequences on cytoskeletal remodeling and cellular division. In our case, it appears that IDE antibody exerted a modest (~20%) inhibition of melanoma cell proliferation.

In prior publications, we have characterized the biosynthesis of the predominant VZV glycoprotein gE in considerable detail (12, 24). Like many other glycoproteins, VZV gE has several distinguishable forms as the protein is synthesized by the polyribosomes and transported into the ER and subsequently through the Golgi stacks into the *trans*-Golgi network (TGN) (Fig. 10). These include a precursor form lacking N-linked oligosaccharides (73 kDa), a form with high-mannose N-linked and O-linked glycans (88 kDa), and a mature form containing both O-linked and N-linked complex-type glycans (98 kDa). In the course of the present investigation, we found that IDE bound the initial nonglycosylated precursor 73-kDa form of gE. Two questions arose from this observation: (i) Why did the other investigations of IDE and VZV interactions fail to detect the precursor form of gE, and (ii) where in the course of the infectious cycle would endogenous IDE encounter the precursor form of gE? Herein we consider these questions in turn.

Other investigations may not have detected the precursor form of gE interacting with IDE for several reasons: first, the interaction is very sensitive to salt concentration; second, different antibodies may not bind all forms of gE equally well; finally, small differences in conditions of SDS-PAGE may lead to an incomplete separation of the large gE/gI complex, with an apparent MW higher than expected (12). We showed that the coprecipitation of VZV gE forms was sensitive to salt concentration in the precipitation buffer. High salt eliminated the coprecipitation totally while low salt led to the coprecipitation of higher-molecular-mass forms of gE in addition to the 73-kDa form. Likely, most forms of gE would coprecipitate at the much lower salt concentration (15 mM) used in prior studies (19). Thus, the binding of the 73-kDa form of gE with IDE would be obscured.

With regard to antibody specificity, we have produced a large library of VZV antibodies that recognize the different forms of VZV gE. The best-characterized antibody against gE is MAb 3B3 (15). This is the only antibody reagent with a fully determined epitope, namely, gE amino acids 150 to 161 (32). The epitope is linear and extremely resistant to blockage or reducing conditions in that the antibody will attach even in the presence of 1% SDS (24). Since the epitope does not require secondary or tertiary structure, the antibody recognizes all gE forms from 73 kDa to 98 kDa (Fig. 10). Furthermore, the association and dissociation constants for the 3B3 antibody have been calculated and are similar to most antibody/epitope affinities (17). We also used a high-titered guinea pig monospecific polyclonal anti-gE antibody in this study. We have

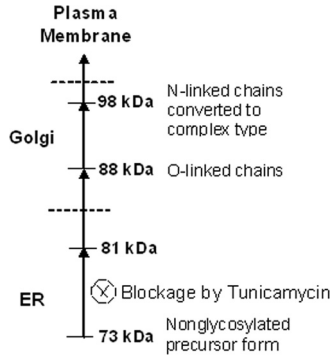

FIG. 10. Oligosaccharide processing of VZV gE. The maturation of VZV gE in the ER and Golgi apparatus of infected cells generates four distinct forms of gE, 73 kDa, 81 kDa, 88 kDa, and 98 kDa, as determined by Montalvo et al. (24).The 73-kDa form is normally processed immediately into the mannosylated 81-kDa form upon synthesis at the ER wall; however, if biosynthesis is blocked by tunicamycin, then the 73-kDa form accumulates in the ER.

observed that the guinea pig anti-gE antibody attached less well to the 73-kDa gE form. Therefore, it is highly likely that other commercial antibodies to VZV gE also attach less well to the 73-kDa form. In the case of glycoproteins, many antibodies recognize conformational epitopes that require at least partial glycosylation. We suggest that differences between antibody reagents have been, in part, responsible for the differing results from prior reports.

The tunicamycin experiments were extremely informative in our validation of the important role of the 73-kDa gE form in the gE-IDE interaction. The easiest method by which to obtain the precursor gE is to grow the virus in the presence of tunicamycin, an inhibitor of complex-type glycosylation in the ER (11, 12). When coprecipitation was carried out with IDE antibody and tunicamycin-treated infected cell lysates, the gE precursor form (73 kDa) was identified (Fig. 10). This is the same form that was preferentially coprecipitated in untreated VZV-infected cells. The 73-kDa gE form is found in the ER in treated infected cells (11). Thus, the coprecipitation reaction occurred between IDE and a gE form found only in the ER. It is highly likely that the site of interaction on gE is the domain previously identified (1). This site is not located near a glycan attachment site and would be available on the precursor form or a glycosylated form (11). In summary, even though smaller amounts of the higher-MW gE forms are also coprecipitated by IDE, we postulate based on the data in this report that IDE primarily interacts with the ER form of gE.

Once we discovered this association with precursor gE, we postulated that the interaction may be related to the cellular pathway known as ER-associated degradation (ERAD). ERAD is a well-established mechanism by which misfolded proteins are retrotranslocated from the ER to the cytosol for degradation (39). Of interest, treatment of cells with tunicamycin can enhance ERAD of misfolded precursor glycoproteins, presumably because tunicamycin blockage results in their accumulation and subsequent ER stress, leading in turn to ERAD (39). Of further interest, ERAD substrates must remain in solution in order for them to be retrotranslocated (26). Molecular chaperones assist in the transportation; one of these is the heat shock protein HSPA5 or BiP (37). As shown in Results, we have detected BiP in a mass spectrometric analysis of purified gE samples. In the same experiment we have also identified two other heat shock proteins (HSPA8 and HSPD1) and a fourth protein (PPIA) commonly associated with ERAD. This result provides further evidence in support of the gE ERAD hypothesis. Further, we have documented that autophagy occurs in VZV-infected cells (36). ER stress is often a precipitating factor for subsequent autophagy (25).

Finally, there is an example of an ERAD substrate that is bound by IDE after translocation from the ER to cytosol (33). That protein is amyloid-β peptide. During Alzheimer's disease, amyloid-β protein is generated by proteolysis of amyloid precursor protein. Some amyloid-β peptide is retrotranslocated by both a proteasome-dependent and a proteasome-independent pathway. The cytosolic enzyme that degrades amyloid-β peptide in the latter pathway is IDE. However, since IDE usually cleaves only small peptides such as insulin and amyloid, any enzymatic effect of IDE on precursor gE as a substrate remains to be determined.

ACKNOWLEDGMENTS

We thank Richard Roller (Iowa) and David Johnson (Oregon) for HSV-1 reagents, as well as valuable advice about carrying out the HSV experiments.

This research was supported in part by NIH grant AI53846.

REFERENCES

1. **Ali, M. A., Q. Li, E. R. Fischer, and J. I. Cohen.** 2009. The insulin degrading enzyme binding domain of varicella-zoster virus (VZV) glycoprotein E is important for cell-to-cell spread and VZV infectivity, while a glycoprotein I binding domain is essential for infection. Virology **386:**270–279.
2. **Bernales, S., F. R. Papa, and P. Walter.** 2006. Intracellular signaling by the unfolded protein response. Annu. Rev. Cell Dev. Biol. **22:**487–508.
3. **Chou, Y. H., W. L. Kuo, M. R. Rosner, W. J. Tang, and R. D. Goldman.** 7 July 2009. Structural changes in intermediate filament networks alter the activity of insulin-degrading enzyme. FASEB J. **23:**3734–3742. [Epub ahead of print.]
4. **de Souza, G. A., H. Malen, T. Softeland, G. Saelensminde, S. Prasad, I. Jonassen, and H. G. Wiker.** 2008. High accuracy mass spectrometry analysis as a tool to verify and improve gene annotation using *Mycobacterium tuberculosis* as an example. BMC Genomics **9:**316.
5. **de Souza, G. A., T. Softeland, C. J. Koehler, B. Thiede, and H. G. Wiker.** 2009. Validating divergent ORF annotation of the *Mycobacterium leprae* genome through a full translation data set and peptide identification by tandem mass spectrometry. Proteomics **9:**3233–3243.
6. **Duckworth, W. C., R. G. Bennett, and F. G. Hamel.** 1998. Insulin degradation: progress and potential. Endocr. Rev. **19:**608–624.
7. **Duus, K. M., C. Hatfield, and C. Grose.** 1995. Cell surface expression and fusion by the varicella-zoster virus gH:gL glycoprotein complex: analysis by laser scanning confocal microscopy. Virology **210:**429–440.
8. **Ejercito, P. M., E. D. Kieff, and B. Roizman.** 1968. Characterization of herpes simplex virus strains differing in their effects on social behaviour of infected cells. J. Gen. Virol. **2:**357–364.
9. **Fawcett, J., and W. C. Duckworth.** 2009. Hyperglycaemia and hyperinsulinaemia: is insulin-degrading enzyme the missing link? Diabetologia **52:**1457–1460.
10. **Friedrichs, W. E., and C. Grose.** 1984. Glycoprotein gp118 of varicella-zoster virus: purification by serial affinity chromatography. J. Virol. **49:**992–996.
11. **Grose, C.** 1990. Glycoproteins encoded by varicella-zoster virus: biosynthesis, phosphorylation, and intracellular trafficking. Annu. Rev. Microbiol. **44:**59–80.
12. **Grose, C.** 2002. The predominant varicella-zoster virus gE and gI glycoprotein complex, p. 195–223. *In* A. Holzenburg, E. Bogner (ed.), Structure-function relationships of human pathogenic viruses. Kluwer Academic/Plenum Publishers, New York, NY.
13. **Grose, C.** 1980. The synthesis of glycoproteins in human melanoma cells infected with varicella-zoster virus. Virology **101:**1–9.
14. **Grose, C., and P. A. Brunel.** 1978. Varicella-zoster virus: isolation and propagation in human melanoma cells at 36 and 32°C. Infect. Immun. **19:**199–203.
15. **Grose, C., D. P. Edwards, W. E. Friedrichs, K. A. Weigle, and W. L. McGuire.** 1983. Monoclonal antibodies against three major glycoproteins of varicella-zoster virus. Infect. Immun. **40:**381–388.
16. **Grose, C., D. M. Perrotta, P. A. Brunell, and G. C. Smith.** 1979. Cell-free varicella-zoster virus in cultured human melanoma cells. J. Gen. Virol. **43:**15–27.
17. **Grose, C., S. Tyler, G. Peters, J. Hiebert, G. M. Stephens, W. T. Ruyechan, W. Jackson, J. Storlie, and G. A. Tipples.** 2004. Complete DNA sequence analyses of the first two varicella-zoster virus glycoprotein E (D150N) mutant viruses found in North America: evolution of genotypes with an accelerated cell spread phenotype. J. Virol. **78:**6799–6807.
18. **Im, H., M. Manolopoulou, E. Malito, Y. Shen, J. Zhao, M. Neant-Fery, C. Y. Sun, S. C. Meredith, S. S. Sisodia, M. A. Leissring, and W. J. Tang.** 2007. Structure of substrate-free human insulin-degrading enzyme (IDE) and biophysical analysis of ATP-induced conformational switch of IDE. J. Biol. Chem. **282:**25453–25463.
19. **Li, Q., M. A. Ali, and J. I. Cohen.** 2006. Insulin degrading enzyme is a cellular receptor mediating varicella-zoster virus infection and cell-to-cell spread. Cell **127:**305–316.
20. **Li, Q., T. Krogmann, M. A. Ali, W. J. Tang, and J. I. Cohen.** 2007. The amino terminus of varicella-zoster virus (VZV) glycoprotein E is required for binding to insulin-degrading enzyme, a VZV receptor. J. Virol. **81:**8525–8532.
21. **Makarov, A.** 2000. Electrostatic axially harmonic orbital trapping: a high-performance technique of mass analysis. Anal. Chem. **72:**1156–1162.
22. **Makarov, A., E. Denisov, A. Kholomeev, W. Balschun, O. Lange, K. Strupat, and S. Horning.** 2006. Performance evaluation of a hybrid linear ion trap/Orbitrap mass spectrometer. Anal. Chem. **78:**2113–2120.
23. **McMillan, T. N., and D. C. Johnson.** 2001. Cytoplasmic domain of herpes simplex virus gE causes accumulation in the *trans*-Golgi network, a site of virus envelopment and sorting of virions to cell junctions. J. Virol. **75:**1928–1940.

24. **Montalvo, E. A., R. T. Parmley, and C. Grose.** 1985. Structural analysis of the varicella-zoster virus gp98-gp62 complex: posttranslational addition of N-linked and O-linked oligosaccharide moieties. J. Virol. **53:**761–770.
25. **Nakatsukasa, K., and J. L. Brodsky.** 2008. The recognition and retrotranslocation of misfolded proteins from the endoplasmic reticulum. Traffic **9:**861–870.
26. **Nakatsukasa, K., G. Huyer, S. Michaelis, and J. L. Brodsky.** 2008. Dissecting the ER-associated degradation of a misfolded polytopic membrane protein. Cell **132:**101–112.
27. **Olsen, J. V., L. M. de Godoy, G. Li, B. Macek, P. Mortensen, R. Pesch, A. Makarov, O. Lange, S. Horning, and M. Mann.** 2005. Parts per million mass accuracy on an Orbitrap mass spectrometer via lock mass injection into a C-trap. Mol. Cell Proteomics **4:**2010–2021.
28. **Olson, J. K., and C. Grose.** 1997. Endocytosis and recycling of varicella-zoster virus Fc receptor glycoprotein gE: internalization mediated by a YXXL motif in the cytoplasmic tail. J. Virol. **71:**4042–4054.
29. **Peters, G. A., S. D. Tyler, C. Grose, A. Severini, M. J. Gray, C. Upton, and G. A. Tipples.** 2006. A full-genome phylogenetic analysis of varicella-zoster virus reveals a novel origin of replication-based genotyping scheme and evidence of recombination between major circulating clades. J. Virol. **80:** 9850–9860.
30. **Qiu, W. Q., and M. F. Folstein.** 2006. Insulin, insulin-degrading enzyme and amyloid-beta peptide in Alzheimer's disease: review and hypothesis. Neurobiol. Aging **27:**190–198.
31. **Rappsilber, J., Y. Ishihama, and M. Mann.** 2003. Stop and go extraction tips for matrix-assisted laser desorption/ionization, nanoelectrospray, and LC/MS sample pretreatment in proteomics. Anal. Chem. **75:**663–670.
32. **Santos, R. A., J. A. Padilla, C. Hatfield, and C. Grose.** 1998. Antigenic variation of varicella-zoster virus Fc receptor gE: loss of a major B cell epitope in the ectodomain. Virology **249:**21–31.
33. **Schmitz, A., A. Schneider, M. P. Kummer, and V. Herzog.** 2004. Endoplasmic reticulum-localized amyloid beta-peptide is degraded in the cytosol by two distinct degradation pathways. Traffic **5:**89–101.
34. **Scigelova, M., and A. Makarov.** 2006. Orbitrap mass analyzer—overview and applications in proteomics. Proteomics **6**(Suppl. 2)**:**16–21.
35. **Shii, K., and R. A. Roth.** 1986. Inhibition of insulin degradation by hepatoma cells after microinjection of monoclonal antibodies to a specific cytosolic protease. Proc. Natl. Acad. Sci. U. S. A. **83:**4147–4151.
36. **Takahashi, M. N., W. Jackson, D. T. Laird, T. D. Culp, C. Grose, J. I. Haynes II, and L. Benetti.** 2009. Varicella-zoster virus infection induces autophagy in both cultured cells and human skin vesicles. J. Virol. **83:**5466–5476.
37. **Tavaria, M., T. Gabriele, I. Kola, and R. L. Anderson.** 1996. A hitchhiker's guide to the human Hsp70 family. Cell Stress Chaperones **1:**23–28.
38. **Tkacz, J. S., and O. Lampen.** 1975. Tunicamycin inhibition of polyisoprenyl *N*-acetylglucosaminyl pyrophosphate formation in calf-liver microsomes. Biochem. Biophys. Res. Commun. **65:**248–257.
39. **Vembar, S. S., and J. L. Brodsky.** 2008. One step at a time: endoplasmic reticulum-associated degradation. Nat. Rev. Mol. Cell Biol. **9:**944–957.